Supplementary Material for New Journal of Chemistry

SUPPLEMENTARY MATERIALS

Formation of Cyano-Bridged Molecule Based Magnetic Nanoparticles within Hybrid Mesoporous Silica.

Guylhaine Clavel, Yannick Guari,* Joulia Larionova,* and Christian Guérin

Laboratoire de Chimie Moléculaire et Organisation du Solide (LCMOS), UMR 5637, Université Montpellier II, Place E. Bataillon, 34095 Montpellier cedex 5, France. Fax: (33) 4 67 14 38 52, e-mail: joulia@univ-montp2.fr; guari@univ-montp2.fr.

Elemental analyses

Figures

Figure 1S. UV-Vis spectra of the bulk compound $Fe_4[Fe(CN)_6]_3$ (-•-) and the nanocomposite **1** (-o-).

Figure 2S. Infrared spectra of a) the hybrid functionalized silica $NC_5H_5(CH_2)_2SiO_{1.5}/11SiO_2$; b) the bulk sample $Fe_4[Fe(CN)_6]_3$; c) the nanocomposite **1**; d) the bulk sample $Ni_3[Fe(CN)_6]_2$; e) the nanocomposite **2**; f) the bulk sample $Fe[Mo(CN)_8]$; g) the nanocomposite **3**; h) the nanocomposite **4**.

Figure 3S. Powder X-ray diffraction patterns within the range of 2Θ (0 – 10°) for the pristine nonfunctionalized silica (-•-), pristine hybrid functionalized silica $NC_5H_5(CH_2)_2SiO_{1.5}/11SiO_2$ (-o-), the nanocomposite 2 (-□-) and the nanocomposite 3 (-♦-). Insert: Magnification of the powder X-ray diffraction patterns showing the (110) and (200) reflections.

Figure 4S. Fe (◊) and Ni (o) atomic contents as inferred from EDS analysis *vs.* the number of impregnation cycles for the successive impregnation of Ni^{2+} and $[Fe(CN)_6]^{3+}$.

Figure 5S. Histogram of nanoparticles size distribution obtained from an extractive replica of the nanocomposite **1**.

Elemental analyses

The pristine functionalized silica $NC_5H_4(CH_2)_2SiO_{1.5}/11SiO_2$. Elemental Anal. calc. for $C_7H_8NO_{23.5}Si_{12}$: Si, 41.03; N, 1.68 %. Found: Si, 33.39; N, 1.41 %. The results of the elemental analyses for Si is lower that the expected theoretical value that is often attributed to the incomplete condensation in the silica framework resulting in the presence of residual alkoxy groups.

Nanocomposites obtained after impregnation of M^{n+} *into* $NC_5H_4(CH_2)_2SiO_{1.5}/11SiO_2$.

Anal. calc. from EDS for $(FeCl_2, 5H_2O)/NC_5H_5(CH_2)_2SiO_{1.5}/11SiO_2$: Fe 5.30 %; Found: Fe 4.97 %.

Anal. calc. from EDS for $(NiCl_2, 5H_2O)/NC_5H_5(CH_2)_2SiO_{1.5}/11SiO_2$: Ni 5.60 %; Found: Ni 4.96 %.

Anal. calc. from EDS for $(FeCl_3, 5H_2O)/NC_5H_5(CH_2)_2SiO_{1.5}/11SiO_2$: Fe 5.00 %; Found: Fe 4.87 %.

Nanocomposites obtained after the third impregnation cycle.

Elemental Anal. found for nanocomposite **1**: Fe 6.96 %; Si 30.06 %.

Elemental Anal. found for nanocomposite **2**: Fe 2.07 %; Ni 2.73 %; Si 33.61 %.

Elemental Anal. found for nanocomposite **3**: Fe 10.58 %; Mo 5.40 %; Si 22.90 %.

Elemental Anal. found for nanocomposite **4**: Ni 3.83 %; Mo 3.90 %; Si 29.31 %.

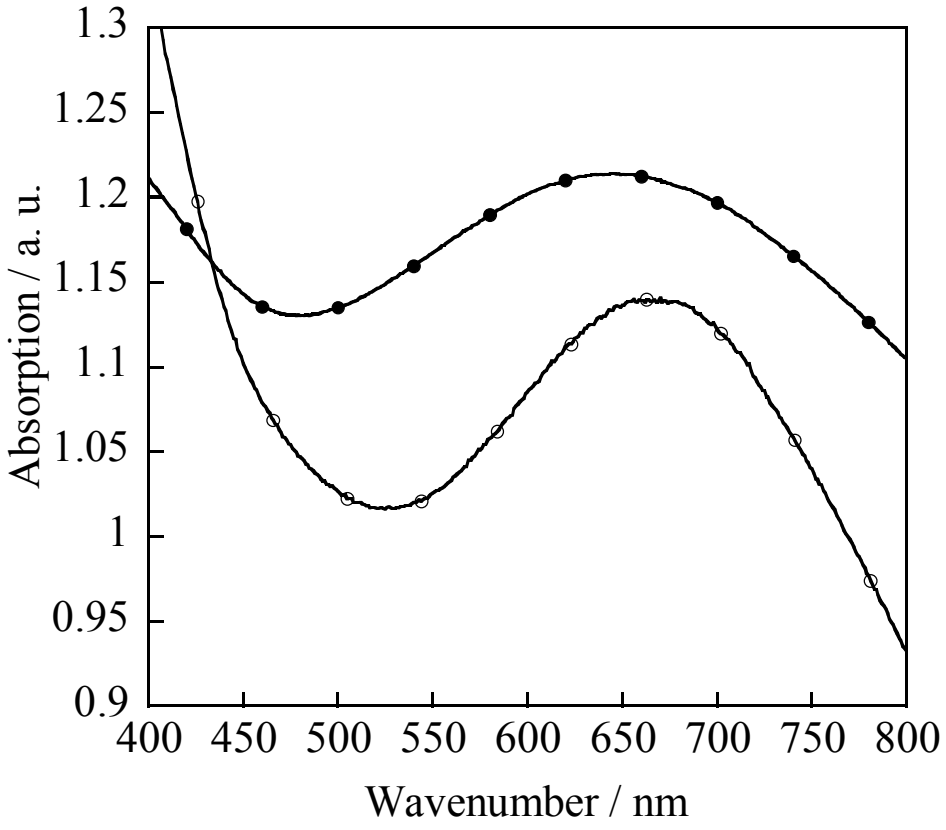

Figure 1S. UV-Vis spectra of the bulk compound $Fe_4[Fe(CN)_6]_3$ (-•-) and the nanocomposite **1 (-o-)**.

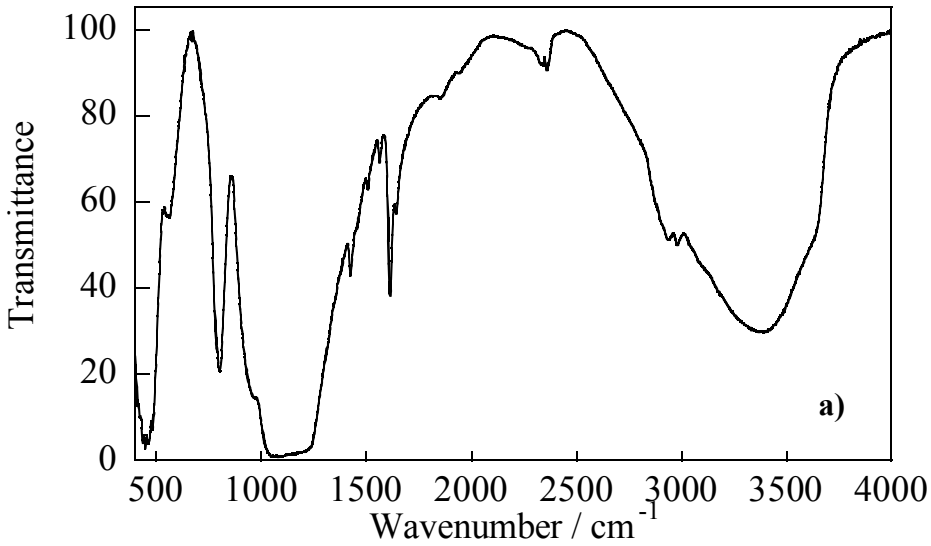

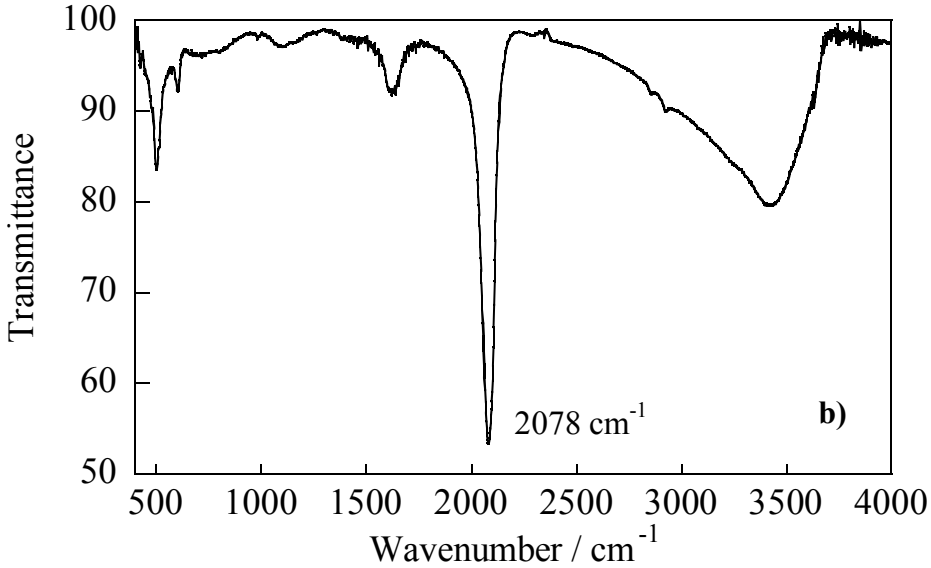

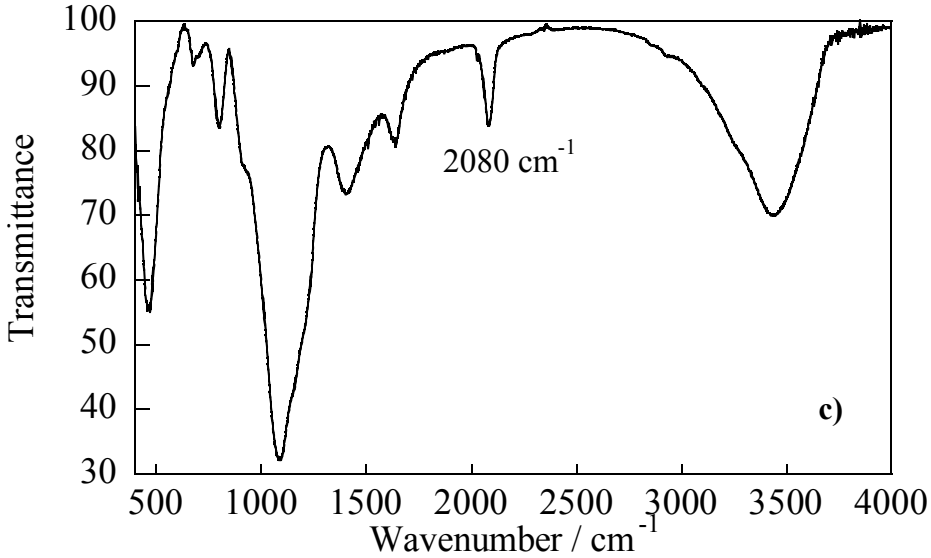

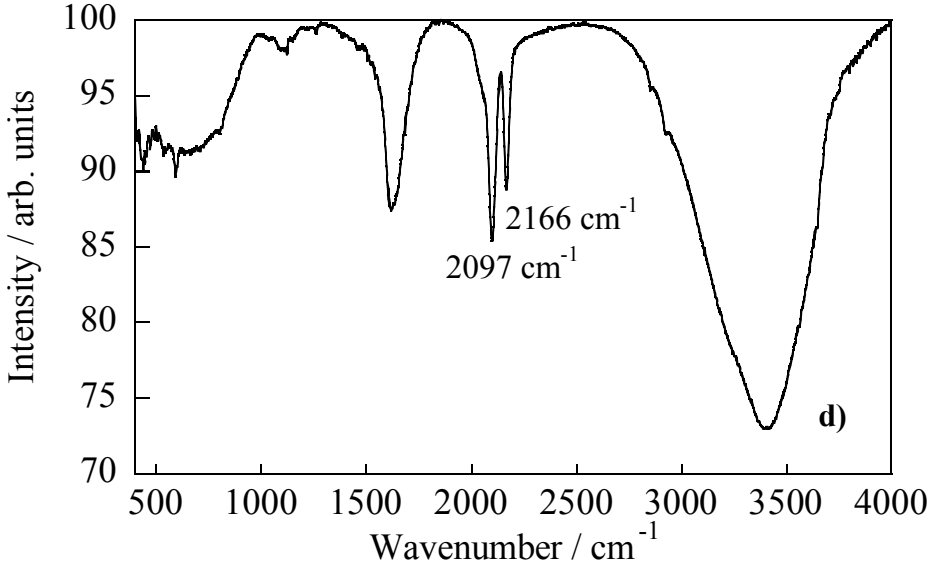

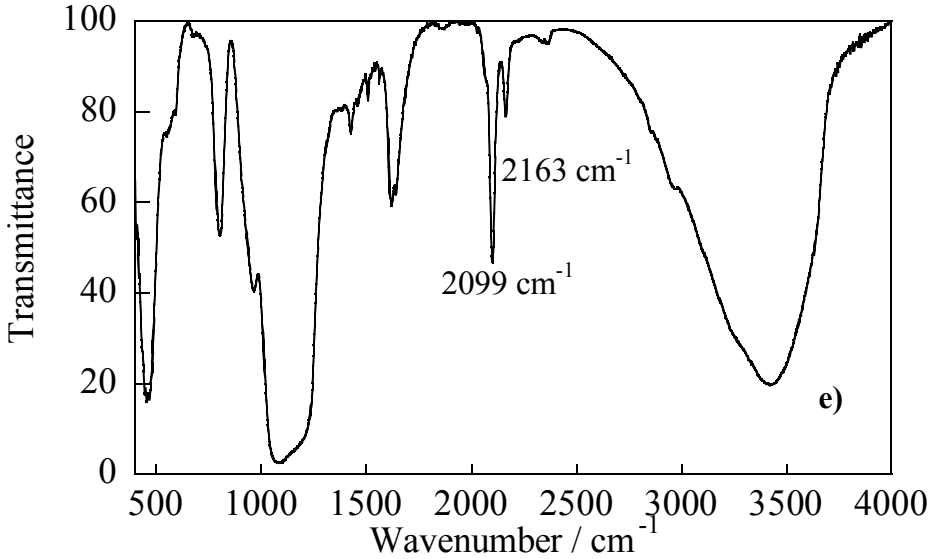

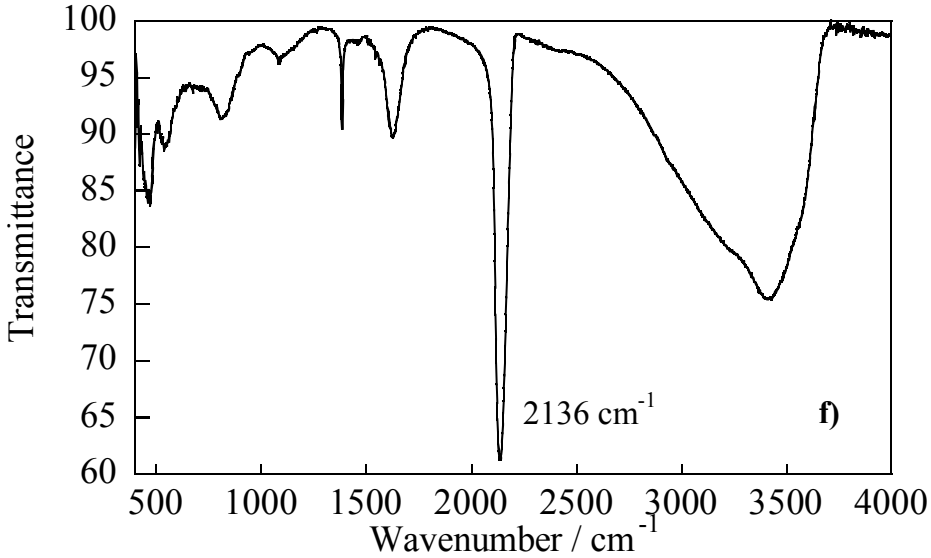

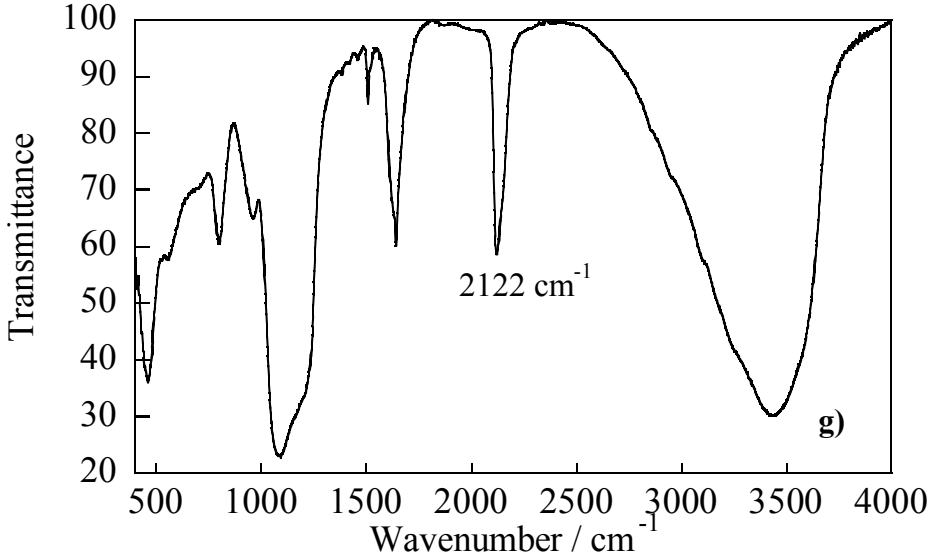

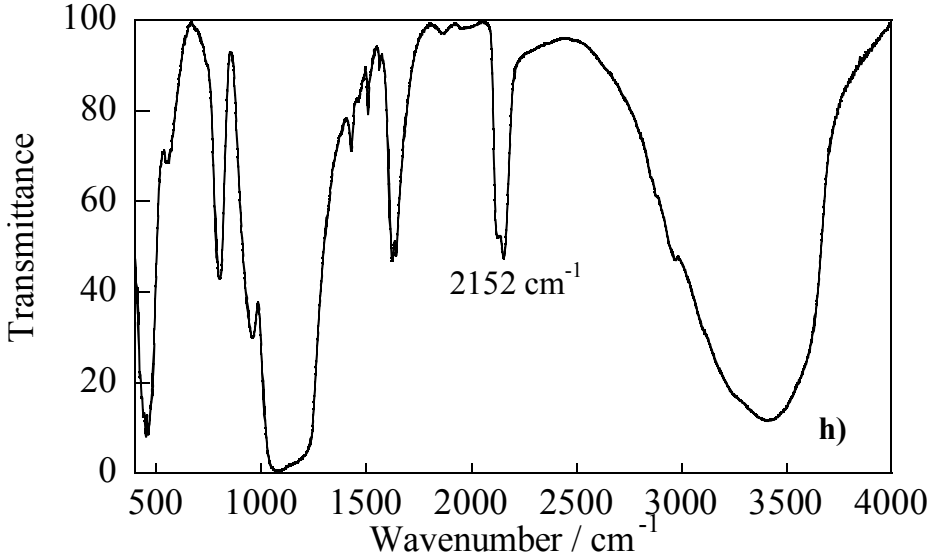

Figure 2S. Infrared spectra of a) the hybrid functionalized silica $NC_5H_5(CH_2)_2SiO_{1.5}/11SiO_2$; b) the bulk sample $Fe_4[Fe(CN)_6]_3$; c) the nanocomposite **1**; d) the bulk sample $Ni_3[Fe(CN)_6]_2$; e) the nanocomposite **2**; f) the bulk sample $Fe[Mo(CN)_8]$; g) the nanocomposite **3**; h) the nanocomposite **4**.

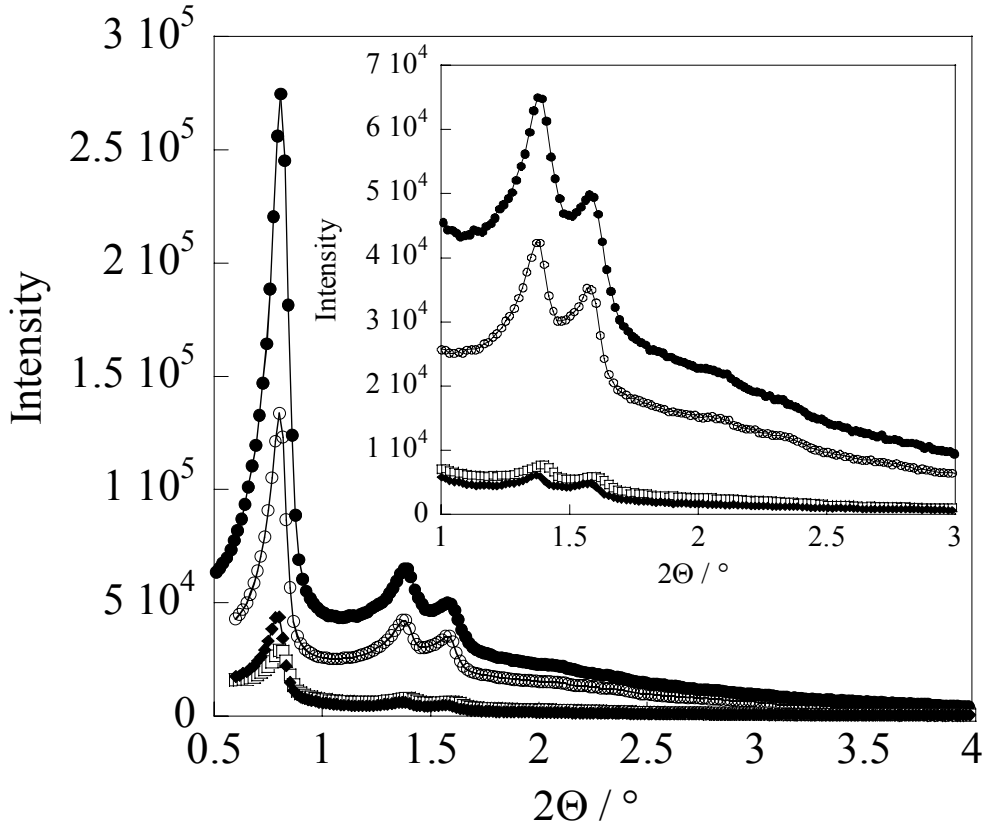

Figure 3S. Powder X-ray diffraction patterns within the range of 2Θ (0 – 10°) for the pristine nonfunctionalized silica (-•-), pristine hybrid functionalized silica $NC_5H_5(CH_2)_2SiO_{1.5}/11SiO_2$ (-o-), the nanocomposite 2 (-□-) and the nanocomposite 3 (-♦-). Insert: Magnification of the powder X-ray diffraction patterns showing the (110) and (200) reflections.

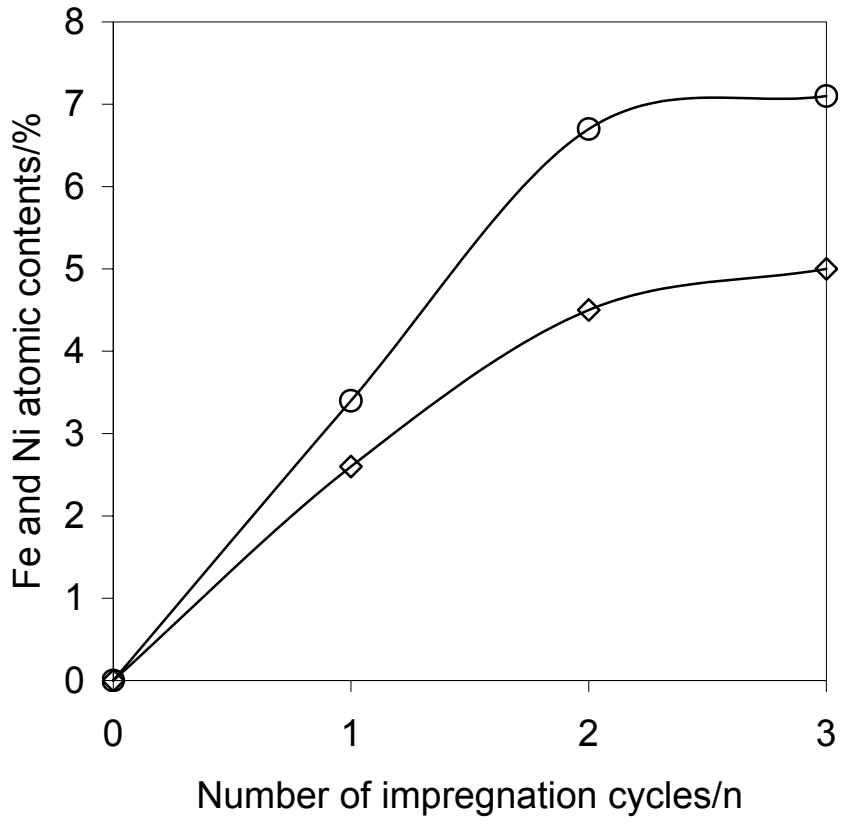

Figure 4S. Fe (◊) and Ni (o) atomic contents as inferred from EDS analysis *vs.* the number of impregnation cycles for the successive impregnation of Ni^{2+} and $[Fe(CN)_6]^{3+}$.

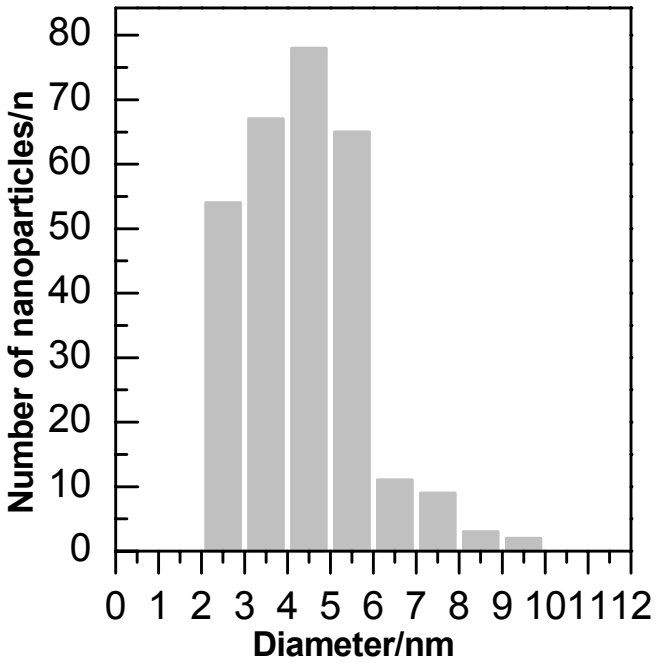

Figure 5S. Histogram of nanoparticles size distribution obtained from an extractive replica of the nanocomposite **1**.